

VAPOR PRESSURE AND DISSOCIATION ENERGY OF (In₂O)

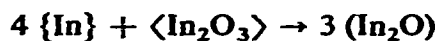
J. VALDERRAMA-N AND K. T. JACOB

Department of Metallurgy and Materials Science, University of Toronto, Toronto M5S 1A4 (Canada)

(Received 20 December 1976)

ABSTRACT

The vapor pressure of pure liquid indium, and the sum of pressures of (In) and (In₂O) species over the condensed phase mixture {In} + <In₂O₃>, contained in a silica vessel, have been measured by Knudsen effusion and Langmuir free vaporization methods in the temperature range 600 to 950°C. Mass spectrometric studies reported in the literature show that (In) and (In₂O) are the important species in the vapor phase over the {In} + <In₂O₃> mixture. The vapor pressure of (In₂O) corresponding to the reaction,



deduced from the present measurements is given by the equation,

$$\log p = - \frac{13,150}{T} + 7.58 (\pm 0.02) \text{ atm}$$

The “apparent evaporation coefficient” for the condensed phase mixture is approximately 0.8. The energy for the dissociation (In₂O) molecule into atoms calculated from the above equation is $D_0^\circ = 180.0 (\pm 1.0) \text{ kcal mol}^{-1}$.

INTRODUCTION

The design of potential fuming processes for the recovery of indium from low-grade raw materials requires accurate knowledge of the vaporization chemistry of indium oxide. Early transpiration study of the vaporization of <In₂O₃> by Shchukarev et al.¹ incorrectly ascribed the weight change to the escape of gaseous (In₂O₃) molecules. The mass spectrometric studies of Burns et al.^{2, 3} on the vaporization of <In₂O₃> from a molybdenum Knudsen cell lined with alumina in the temperature range 1000 to 1265°C suggest that (In), (O₂) and (In₂O) are the only important species. They^{2, 3} estimate a “third law” atomization energy of $D_0^\circ = 179 (\pm 4) \text{ kcal mol}^{-1}$ for (In₂O). To derive pressures from ion intensities, imprecise calibration procedures based on quantitative silver evaporation and literature values for the relative ionization cross sections were used. More recently, Shchukarev et al.⁴ have studied the vaporization of pure <In₂O₃> from 1250 to 1350°C, and a mixture of

{In} + <In₂O₃> from 750 to 825°C, by mass spectrometric analysis of the vapors effusing from molybdenum Knudsen cells lined with alumina. The pressure of In₂O over the condensed phase mixture was obtained by following the time dependence of the ion intensity of (In₂O⁺) accompanying the complete vaporization of the mixture and using the formula,

$$p = I^+ T \left[\frac{w}{B \int_0^t I^+ dt} \right] \quad (1)$$

where $B = A \sqrt{MT}/2\pi R$. Sufficient information is not available to critically assess the accuracies obtainable by this technique, especially for a two-phase system. The second and third law heats of atomization of (In₂O) at 298 K obtained by Shchukarev et al.⁴ are 185.5 (± 3) and 193.5 (± 2) kcal mol⁻¹, respectively. Because of the significant discrepancy in the third-law values for the atomization energy of (In₂O) obtained from the two mass spectrometric studies, the vapor pressure of pure indium and the total pressure over {In} + <In₂O₃> mixture were measured in this study using the Knudsen and Langmuir methods. The comparison of the values obtained by the two techniques would provide information on the "apparent evaporation coefficient" for {In} + <In₂O₃> mixture, which is a measure of the kinetics of the heterogeneous reaction at the phase boundary.

EXPERIMENTAL METHODS

Materials

Silver and indium metals, each 99.995% pure, were obtained from Cominco and Ventron Corporation, respectively, in granular form. Indium sesquioxide powder of optical purity (99.999%) was supplied by Ventron Corporation.

Apparatus and procedure

The rates of weight loss of Knudsen and Langmuir cells were measured by a high vacuum Anisworth analytical balance (AV-1) provided with an electronic indicating and recording device. The balance was capable of measuring weight changes up to 200 mg with 0.1 mg sensitivity. A schematic diagram of the apparatus is shown in Fig. 1. The heating element of the vacuum furnace was a cylindrical tungsten mesh sleeve, 0.13 mm thick and having 16 holes per cm. The molybdenum tubes and discs provided the radiation shielding system. Strips of zirconia slab were used for thermal insulation between the outer radiation shield and the water-cooled stainless-steel shell of the furnace. Power was supplied to the heater from an air-cooled transformer. The maximum operating temperature of the furnace was 1200°C and the temperature could be controlled to $\pm 2^\circ\text{C}$. The temperature inside the furnace was measured by a Pt-Pt (13% Rh) thermocouple calibrated, before and after the experiments, against the melting point of gold. The vacuum system consisted of an oil

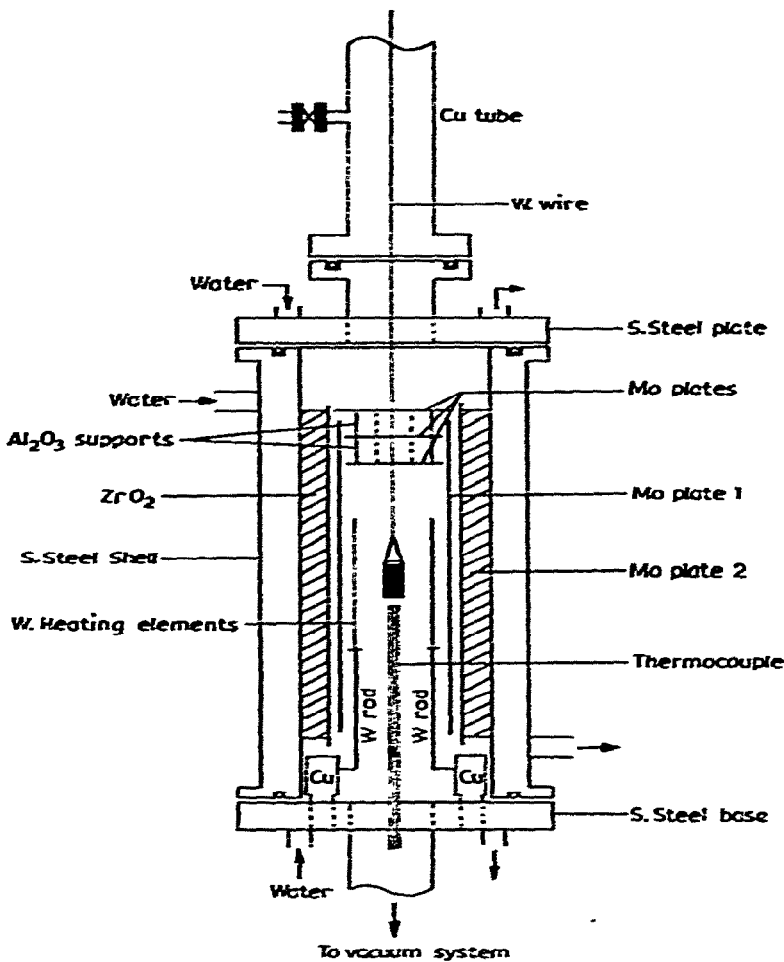


Fig. 1. Schematic diagram of the apparatus.

diffusion pump backed by a mechanical rotary pump. A typical pressure in the furnace during most of the measurements was 10^{-8} atm.

The Knudsen effusion cells made of quartz were 2 cm long and 0.8 cm in diameter. The wall thickness of the quartz cell was 1 mm. A small area (3×3 mm) on the upper lateral side of the silica cell was ground by a diamond tool till the wall thickness was approximately 0.2 mm. A Knudsen orifice was drilled in the center of this area of reduced thickness with an ultrasonic drill and silicon carbon abrasive slurry. The diameter of the orifice was measured by a Dynazoom optical microscope provided with a sensitive internal scale that could be superimposed on the orifice image. The nominal orifice diameter at the experimental temperature was calculated from that at room temperature by using a value of $5.5 \times 10^{-7}/K$ for the thermal expansion coefficient of silica. The "effective orifice area" of the cell was calculated from the measured rate of weight loss of a cell containing pure silver and values for the vapor pressure of silver given in the compilation of Hultgren et al.⁵. It was found

that the nominal and effective orifice areas were identical ($\pm 2\%$), indicating that the Clausing factor for the orifice was unity.

The Langmuir cells were identical to the Knudsen cells except that the top of the cell was open to vacuum. The inner diameter of the silica cell was used to compute the evaporation area. The cells were suspended from one arm of the balance by a tungsten wire. The length of the wire was adjusted to keep the cell in the uniform temperature zone of the furnace. The distance between the cell and the thermocouple was about 1 mm.

RESULTS

The orifice area, temperature, and the rate of weight loss of the silica Knudsen cells containing {In} or a mixture of {In} + $\langle \text{In}_2\text{O}_3 \rangle$ are summarized in Tables 1 and 2. The vapor pressure is calculated using the Knudsen equation,

$$p = 0.02256 \frac{m}{t \cdot A} \sqrt{\frac{T}{M}} \quad (2)$$

The vapor pressure of pure indium obtained from the measurements are also shown in Table 1. The logarithm of the vapor pressure is plotted against the reciprocal of absolute temperature in Fig. 2. The least-mean-squares regression analysis suggests the following equation for the vapor pressure of pure indium;

$$\log p = -\frac{11,900}{T} + 5.08 (\pm 0.02) \text{ atm} \quad (3)$$

This equation is almost identical to that obtained earlier⁶ using graphite Knudsen cells. The standard free energy of vaporization of indium can be calculated from the vapor pressure as follows:

$$\begin{aligned} \{\text{In}\} &\rightarrow (\text{In}) \\ \Delta G^\circ &= -RT \ln K = -RT \ln p \\ &= 54,450 - 23.23T (\pm 150) \text{ cal} \end{aligned} \quad (4)$$

TABLE 1

KNUDSEN EFFUSION STUDY OF THE VAPOR PRESSURE OF PURE INDIUM

orifice area (cm ²)	T (K)	$\Delta w/\Delta t$ (mg sec ⁻¹)	p_{In} (atm)
2.23×10^{-3}	1275	1.64×10^{-3}	5.51×10^{-5}
2.23×10^{-3}	1188	3.52×10^{-4}	1.14×10^{-5}
2.23×10^{-3}	1128	1.06×10^{-4}	3.36×10^{-6}
2.23×10^{-3}	1101	5.96×10^{-5}	1.86×10^{-6}
2.23×10^{-3}	1065	2.59×10^{-5}	7.98×10^{-7}
1.36×10^{-3}	1251	6.68×10^{-4}	3.66×10^{-5}
1.36×10^{-3}	1202	2.78×10^{-4}	1.50×10^{-5}
1.36×10^{-3}	1148	9.72×10^{-5}	5.11×10^{-6}

TABLE 2

KNUDSEN EFFUSION MEASUREMENT OF THE VAPORIZATION OF $\{In\} + \langle In_2O_3 \rangle$ MIXTURE

Orifice area (cm^2)	T (K)	Δw (total) (mg)	$\Delta w/\Delta t$ (total) (mg sec $^{-1}$)	$\Delta w/\Delta t$ (In_2O) (mg sec $^{-1}$)	p_{In_2O} (atm)
2.23×10^{-3}	1202	7.0	1.92×10^{-2}	1.86×10^{-2}	4.16×10^{-4}
2.23×10^{-3}	1134	5.0	4.39×10^{-3}	4.27×10^{-3}	9.26×10^{-5}
2.23×10^{-3}	1098	5.0	1.95×10^{-3}	1.89×10^{-3}	4.04×10^{-5}
2.23×10^{-3}	1055	4.0	6.24×10^{-4}	6.04×10^{-4}	1.26×10^{-5}
2.23×10^{-3}	1024	2.0	2.66×10^{-4}	2.56×10^{-4}	5.29×10^{-6}
2.23×10^{-3}	946	1.8	2.54×10^{-5}	2.43×10^{-5}	4.81×10^{-7}
1.36×10^{-3}	1215	5.0	1.62×10^{-2}	1.59×10^{-2}	5.87×10^{-4}
1.36×10^{-3}	1141	3.0	3.38×10^{-3}	3.30×10^{-3}	1.18×10^{-4}
1.36×10^{-3}	990	5.0	6.18×10^{-5}	5.95×10^{-5}	1.94×10^{-6}

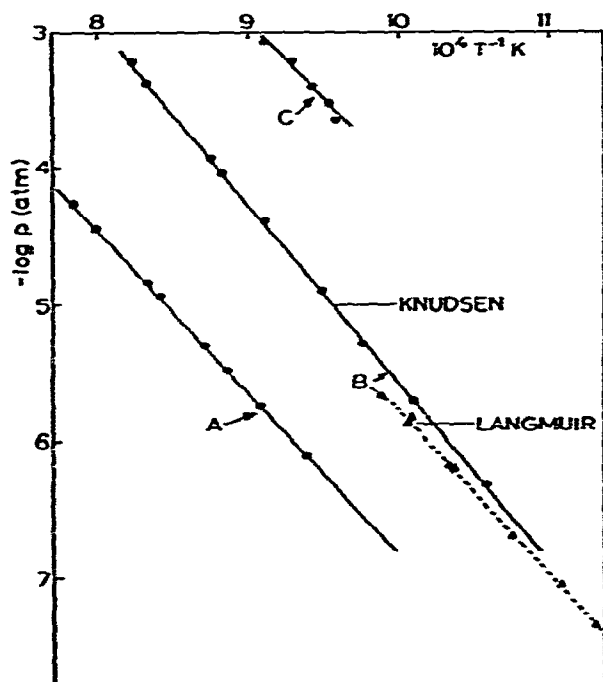


Fig. 2. Vapor pressure of (In) and (In_2O) shown as a function of the reciprocal of absolute temperature. A = equilibrium vapor pressure over pure liquid indium; B = equilibrium partial pressure of (In_2O) over $\{In\} + \langle In_2O_3 \rangle$ mixture, obtained in this study. C = equilibrium partial pressure of (In_2O) over $\{In\} + \langle In_2O_3 \rangle$ measured by Shchukarev et al.⁴

The most significant vapor species over the condensed phase mixture, $\{In\} + \langle In_2O_3 \rangle$, is $(In_2O)^4$. The partial vapor pressure of indium over this mixture is the same as that over pure $\{In\}$. The concentration of other species such as (InO) are less than 1%. The rate of weight loss due to the escape of (In) gas molecules from the Knudsen cell can therefore be subtracted from the total measured weight loss to give the rate of weight loss due to the escape of (In_2O) gas molecules. The vapor pressure

of (In_2O) over the condensed phase mixture obtained in this study is shown in Table 2 and plotted in Fig. 2. The vapor pressure of In_2O corresponding to the reaction,



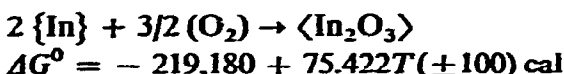
is given by,

$$\log p = - \frac{13,150}{T} + 7.58 (\pm 0.02) \text{ atm} \quad (6)$$

The standard free energy change for reaction (5) is therefore represented by the relation,

$$\begin{aligned} \Delta G_{(5)}^0 &= -RT \ln K = -RT \ln (P_{\text{In}_2\text{O}})^3 \\ &= 180,500 - 104.0T (\pm 350) \text{ cal} \end{aligned} \quad (7)$$

When the above equation is combined with the standard free energy of formation of $\langle \text{In}_2\text{O}_3 \rangle$, obtained from a recent e.m.f. study⁷ using solid oxide galvanic cell,



and the free energy of vaporization of pure indium (eqn. (4)), one obtains for the reaction:



The rate of weight loss of Langmuir cells containing the $\{\text{In}\} + \langle \text{In}_2\text{O}_3 \rangle$ mixture at different temperatures is shown in Table 3. The vapor pressure of In_2O calculated using the expression,

$$p = 0.02256 \frac{m}{t - a - \alpha} \sqrt{\frac{T}{M}} \quad (9)$$

assuming $\alpha = 1$, and after subtracting the contribution to the weight loss due to the escape of indium atoms, is shown in Table 3 and compared with Knudsen measure-

TABLE 3

LANGMUIR EFFUSION MEASUREMENT OF THE VAPORIZATION OF $\{\text{In}\} + \langle \text{In}_2\text{O}_3 \rangle$ MIXTURE

Evaporation area (cm^2)	T (K)	Δw (total) (mg)	$\Delta w/\Delta t$ (total) (mg sec^{-1})	$\Delta w/\Delta t$ (In_2O) (mg sec^{-1})	$P_{\text{In}_2\text{O}}$ (atm)
3.85×10^{-1}	1077	7	3.69×10^{-2}	3.52×10^{-2}	4.22×10^{-6}
3.85×10^{-1}	994	8	1.26×10^{-2}	1.18×10^{-2}	1.39×10^{-6}
3.85×10^{-1}	993	8	1.33×10^{-2}	1.26×10^{-2}	1.49×10^{-6}
3.85×10^{-1}	967	4	5.87×10^{-3}	5.52×10^{-3}	6.42×10^{-7}
3.85×10^{-1}	965	4	5.70×10^{-3}	5.38×10^{-3}	6.25×10^{-7}
3.85×10^{-1}	930	3	1.86×10^{-3}	1.75×10^{-3}	1.99×10^{-7}
3.85×10^{-1}	903	3	8.37×10^{-4}	7.89×10^{-4}	8.87×10^{-8}
3.85×10^{-1}	885	2	4.33×10^{-4}	4.06×10^{-4}	4.52×10^{-8}

ments in Fig. 2. The pressures obtained by the Langmuir method are lower than those obtained by the Knudsen technique, and the difference between the two sets of measurements increases with temperature. Because of the convex nature of the surface of liquid indium in the silica cell, the effective vaporization area is larger than the diameter of the silica cell. It is difficult to accurately estimate the increased area in the absence of data on the surface tension or contact angle between oxygen-saturated liquid indium and silica. However, surface tension may be expected to decrease with increasing temperature, so that the curvature of the liquid surface will be larger and the evaporation will be smaller at higher temperatures. This probably explains the greater difference between Langmuir and Knudsen measurements at the higher temperatures. Although the results of the Langmuir studies are not used to derive thermodynamic data, a value of 0.8 for the "effective evaporation coefficient" of $\{\text{In}\} + \langle \text{In}_2\text{O}_3 \rangle$ mixture can be evaluated by comparison with the Knudsen measurements.

DISCUSSION

The vapor pressures of (In_2O) over the condensed phase mixture $\{\text{In}\} + \langle \text{In}_2\text{O}_3 \rangle$ obtained in this study are lower, by approximately a factor of 20, than those reported by Shchukarev et al.⁴, as shown in Fig. 2. When information is available on the composition of the vapor phase, the Knudsen technique is more reliable than the mass spectrometric technique of Shchukarev et al., in which the time-dependence of ion intensity for complete evaporation of the two-phase mixture is monitored. There are a number of experimental and theoretical problems in delineating the integral, $\int_0^t I^+ dt$, during the final stage of evaporation of a two-phase mixture. Although this technique has been successfully applied to the determination of the vapor pressure of homogeneous single phases⁸ such as $\langle \text{ZrF}_4 \rangle$, the comparison of the vapor pressures in Fig. 2 suggests that it is unsuitable for the determination of the vapor pressure of condensed phase mixtures.

Burns³ has calculated the free energy function, $(G^\circ - H_0^\circ/T)$, for (In_2O) by assuming a bent (145°) symmetric structure by comparison with (Al_2O) and (Ga_2O) , and estimating the interatomic distance (In-O) as 1.97 Å and vibrational frequencies as 710, 130 and 390 cm^{-1} . The free energy functions for In and O_2 are given in the compilation of Hultgren et al.⁵ and Janaf tables⁹, respectively. A "third-law" analysis of the vapor pressure values obtained in the present study is presented in Table 4. The good agreement between the second and third law heats of formation of (In_2O) suggests that the estimated free energy functions for (In_2O) are free from significant error. The value for the energy required to dissociate (In_2O) into atoms obtained from the results of this study is compared with those obtained from mass spectrometric studies in Table 5. The dissociation energy of oxygen molecule is taken from Janaf tables⁹. Considering the large uncertainty in relating ion intensity to absolute pressure, the dissociation energy obtained by Burns et al.^{2, 3} is in good

TABLE 4

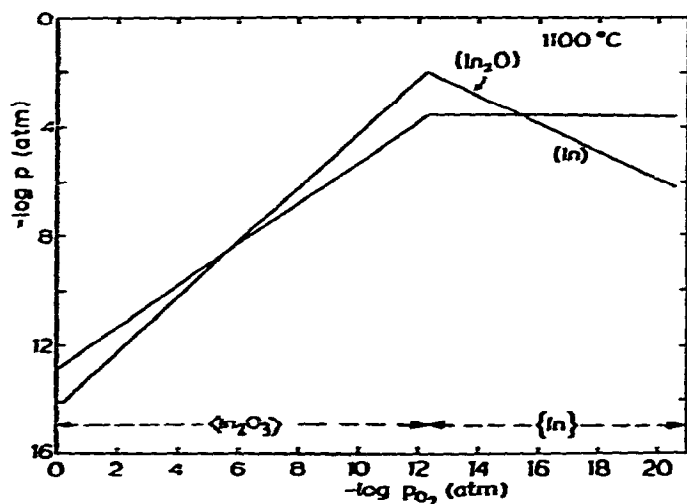
THE STANDARD FREE ENERGY AND ENTHALPY CHANGE FOR THE REACTION $2(\text{In}) + \frac{1}{2}(\text{O}_2) \rightarrow (\text{In}_2\text{O})$

T (K)	$-\Delta G^\circ$ (cal)	Third law	$-\Delta H^\circ_0$ (cal)	Second law
		$-\Delta H^\circ_{298}$ (cal)		$-\Delta H^\circ_{1050}$ (cal)
1202	77,300	122,060	121,110	
1134	79,850	121,960	121,010	
1098	81,270	121,970	121,030	
1055	82,770	121,830	120,900	121,800
1024	83,920	121,780	120,830	
946	86,900	121,770	120,840	
1215	77,000	122,270	121,340	
1141	79,760	122,130	121,200	
990	85,200	121,760	120,820	
Average values		121,950	121,000	121,800

TABLE 5

COMPARISON OF THE DISSOCIATION ENERGY OF (In_2O) OBTAINED IN DIFFERENT STUDIES BY THE "THIRD-LAW" METHOD

Ref.	D°_0 (kcal mol ⁻¹)
Burns et al. ^{2, 3}	179.2 (± 4)
Shchukarev et al. ⁴	191.9 (± 2)
This study	180.0 (± 1)

Fig. 3. The variation of the partial pressures of (In) and (In_2O) in the In-O system with the oxygen partial pressure at 1100°C .

agreement with that deduced from the Knudsen effusion measurements. The value suggested by Shchukarev et al.⁴ appears to be an error.

Since solid indium sesquioxide evaporates with a change in stoichiometry, according to the reaction,



its vapor pressure and hence the rate of vaporization is a function of the partial pressure of oxygen in the ambient atmosphere. The formation of (In_2O) is favored by low oxygen partial pressure. The vapor pressure of (In) over indium sesquioxide is determined by the reaction,



again the indium pressure increases as the oxygen partial pressure is decreased, until the oxygen partial pressure corresponding to the reduction of indium sesquioxide to liquid indium is reached. Since pure liquid indium is formed, a further reduction in oxygen potential does not affect the vapor pressure of (In) . The partial pressure of (In_2O) decreases with the decrease in oxygen potential below that at which $\{\text{In}\}$ and $\langle \text{In}_2\text{O}_3 \rangle$ coexist. Figure 3 shows the variation of the partial pressures of (In) and (In_2O) with the partial pressure of oxygen in the In-O system at 1100°C. In vacuum or inert gas atmosphere, the volatility is restricted by the requirement that $p_{\text{O}_2} = 3/4 p_{\text{In}}$. The total pressure over the In-O system given by,

$$P_T = p_{\text{In}} + p_{\text{In}_2\text{O}} + p_{\text{O}_2} \quad (12)$$

is plotted as a function of oxygen partial pressure at 1100, 1200 and 1300°C in Fig. 4. The pressure of indium containing vapor species at 1300°C has a maximum value of 0.17 atm at the oxygen potential corresponding to the reduction of $\langle \text{In}_2\text{O}_3 \rangle$ to $\{\text{In}\}$. Therefore, rapid fuming of low-grade oxide ores can be achieved at temperatures near 1300°C and with careful control of the oxygen partial pressure in the gas phase.

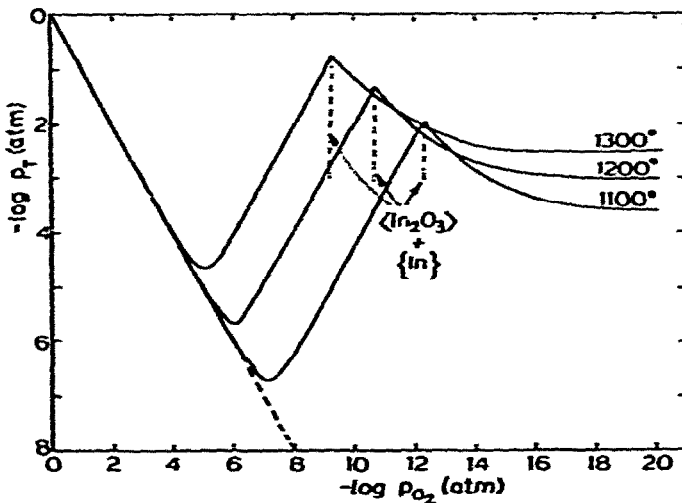


Fig. 4. The total pressure in the In-O system as a function of the oxygen partial pressure.

The oxygen potential of the gas can be controlled by adjusting either the hydrogen-to-steam ratio or the carbon monoxide-to-carbon dioxide ratio. The advent of cheap and reliable solid oxide probes for continuous measurement of oxygen potential in commercial high temperature furnaces, has enabled the attainment of high efficiency for such processes.

NOMENCLATURE

<i>Symbol</i>	<i>Meaning</i>	<i>Units</i>
< >	solid state	
{ }	liquid state	
()	gaseous state	
α	evaporation coefficient	
A	area of Knudsen orifice	cm ²
I^+	ion intensity	
M	molecular weight	g
R	gas constant	cal K ⁻¹ mol ⁻¹
T	absolute temperature	K
a	evaporation area	cm ²
m	weight loss	g
p	pressure	atm
t	time	sec.
w	weight	g
ΔG°	standard Gibbs' free energy change	cal mol ⁻¹ , or kcal mol ⁻¹
ΔH_T°	heat of formation at temperature T	cal mol ⁻¹ , or kcal mol ⁻¹
D_T°	energy for the dissociation of a molecule into atoms (atomization energy) at temperature T	kcal mol ⁻¹

REFERENCES

- 1 S. A. Shchukarev, G. A. Semenov, I. A. Rat'kovskii and V. A. Perevoshchikov, *Zh. Obshch. Khim.*, 31 (1961) 2090.
- 2 R. P. Burns, G. DeMaria, J. Drowart and M. G. Inghram, *J. Chem. Phys.*, 38 (1963) 1035.
- 3 R. P. Burns, *J. Chem. Phys.*, 44 (1966) 3307.
- 4 S. A. Shchukarev, G. A. Semenov and I. A. Rat'kovskii, *Russ J. Inorg Chem.*, 14 (1969) 1.
- 5 R. Hultgren, P. D. Desai, D. T. Hawkins, M. Gleiser, K. K. Kelley and D. D. Wagman, *Selected Values of the Thermodynamic Properties of the Elements*, Am. Soc. Metals, Metals Park, Ohio, 1973.
- 6 J. Valderrama-N, *M. A. Sc. Thesis*, University of Toronto, Toronto, Canada, Oct. 1976.
- 7 K. T. Jacob, *Trans. Inst. Min. Met. (London)*, Sec. C, to be published.
- 8 C. B. Alcock, K. T. Jacob and S. Zador, in *Zirconium: Physico-chemical Properties of its Compounds and Alloys*, Atomic Energy Review, Special Issue No. 6, I. A. E. A., Vienna, 1976.
- 9 D. R. Stull and H. Prophet et al., *JANAF Thermochemical Tables*, NSRDS-NBS 37, 1971.